Egyptian Journal of Veterinary Sciences

https://ejvs.journals.ekb.eg/

Assessment of Anticancer Effect of Anthraquinones on Human Colorectal and Breast Cancer Cells

Mustafa I. ElSawy[1], Mohamed Amr El-Missiry[1], Maggie E. Amer [1] and Mohammed A. El-Magd[2*]

[1]*Zoology Department, Faculty of Science, Mansoura University, Mansoura, Egypt. Drmustafaelsawy@gmail.com (M.I.E), elmissiry@mans.edu.eg (M.A.E), maggieelsied@mans.edu.eg (M.E.A).*

[2]*Anatomy Department, Faculty of Veterinary Medicine, Kafrelsheikh University, 33516, Egypt.*

Abstract

CISPLATIN (Cis) is extensively utilized as an anticancer agent against various types of cancers, including liver, breast, colorectal, and pancreatic cancers. Nevertheless, its application is constrained by its associated side effects including lack of selectivity and DNA damage of both cancerous and healthy cells. This study aimed to investigate the therapeutic impact of anthraquinones (Ant) extracted from Rhubarb officinale against colorectal cancer $CaCO_2$ and breast cancer MCF7 cells. The cells were divided into: untreated control group, Ant-treated group, Cis-treated group and Ant+Cis-treated group. Treatment with Ant and/or Cis triggered MCF7 and $CaCO_2$ apoptosis as revealed by a significant increase in caspase-3 activity, Bax gene expression and a significant reduction in Bcl2 expression. This treatment also downregulated TNFα, VEGF, MMP9 expression while upregulated TIMP1 expression. Regarding the oxidative stress, combined therapy increased the activities of the antioxidant enzymes (SOD, CAT, GPX) and the expression of NrF2 and HO-1. The study concludes that combination of Ants and Cis effectively enhances cisplatin-antitumor efficacy while reducing its chemotherapy-induced toxicity and maintaining safety.

Keywords: Anthraquinones, Cisplatin, $CaCO_2$, MCF7, Apoptosis.

Introduction

Cancer, a complex and multistep process marked by unregulated cell proliferation, represents a substantial global health challenge [1,2]. This challenge is anticipated to intensify due to factors such as aging, escalating obesity prevalence, and ongoing exposure to carcinogenic agents [3]. Although there have been notable advances, understanding and addressing the multifaceted origins and progression of cancer, rooted in complex genetic and epigenetic changes, continues to pose a major scientific challenge [4]. Understanding the molecular foundation of cancer is fundamental to developing effective preventive and therapeutic strategies [5]. Cisplatin (Cis) is a widely utilized chemotherapeutic agent, however, its clinical utility is significantly constrained by severe side effects [2,6]. This limitation arises from its lack of selectivity for cancer cells, as it interacts with the DNA of both cancerous and healthy cells [7]. The co-administration of Cis with natural products that exhibit anticancer activity through diverse mechanisms of action presents a promising strategy to control Cis adverse effects while maintaining or even enhancing its chemotherapeutic efficacy. Anthraquinones (Ant) derived from Rhubarb officinale leaf extract, rich in emodin, aloe-emodin, physcion, and chrysophanol had the potential to inhibit cancers proliferation without impacting the growth of normal (non-cancerous) cells [8]. Ant exerts their anti-cancer effects through diverse mechanisms, targeting various cellular processes: induction of apoptosis, inhibition of cell proliferation [9], ROS induction [10], suppression of angiogenesis and immunomodulatory effects [11]. In contrast to previous studies that examined only a subset of derivatives [8-11], this research presents a comprehensive analysis of the entire spectrum of Ant derivatives in combination with Cis. We proposed that Ant could serve as an effective adjuvant to Cis, enhancing its therapeutic efficacy and reducing its side effects. Accordingly, the present study aimed to investigate the therapeutic impact of Ants against colorectal cancer $CaCO_2$ and breast cancer MCF7 cells.

* Corresponding author: Mohamed A.El-Magd, E-mail: mohamed.abouelmagd@vet.kfs.edu.eg, Tel.: 002 01068160301
(Received 16 April 2025, accepted 04 June 2025)
DOI: 10.21608/ejvs.2025.376009.2792

Material and Methods

Isolation of total anthraquinones from Rhubarb officinale

Total anthraquinones were extracted from Rhubarb officinale as previously detailed [12]. In brief, 2 kg of Rhubarb officinale powder underwent acid hydrolysis by refluxing with 4 L of 10% HCl for 2 hours. Following filtration and drying, the powder was subjected to exhaustive extraction using methylene chloride until a negative result was obtained with Bornträger's test. The methylene chloride was then evaporated under vacuum, and the resulting residue was dissolved in 1 L of 10% sodium carbonate (Na_2CO_3) solution, treated three times, and concentrated under vacuum. The pH was gradually adjusted to 6 by the stepwise addition of diluted HCl, leading to the formation of a heavy yellowish-brown precipitate. This precipitate was collected, dried under vacuum, and yielded 20 g of yellowish-brown powder. Thin-layer chromatography (TLC) analysis of the methylene chloride fraction, using a light petroleum-ethyl acetate-formic acid solvent system (75:25:1) as the mobile phase, revealed four major spots at Rf values ranging from 0.3 to 0.7, indicating the presence of the four primary anthraquinone aglycones.

Cell line and cell culture

Human breast cancer (MCF7) and colorectal adenocarcinoma ($CaCO_2$) cell lines, along with normal kidney cells (Vero), purchased from the US-based cell bank (ATCC, NY, USA) via Vacsera (Egypt). Cells were maintained in DMEM supplemented with 10% heat-inactivated fetal bovine serum (GIBCO, USA) and 1% penicillin/streptomycin (Thermo Fisher Scientific, USA). The cells were then seeded in T25 cm^2 flasks and underwent incubation at 37°C with 5% CO_2. The cultivation medium was renewed at two-day intervals until 80–90% of the cells were confluent. For sub culturing, three rounds of sterile phosphate-buffered saline (PBS, with a pH adjusted to 7.4) washings were performed on the cells. after the removal of the culture medium. Trypsinization was performed by adding 0.025% trypsin-EDTA, and the cells were incubated for 3–5 minutes until detachment was observed. The dissociated cells were then resuspended in fresh DMEM for further cultivation.

Cellular cytotoxicity determination by MTT assay

The possibility of cytotoxicity of total Ant compared to the standard chemotherapeutic agent Cis was assessed in $CaCO_2$, MCF7, and Vero cells using the MTT assay as previously described [13]. Cells (1× 104 /well) were cultured at 37 °C and 5% CO_2 for twenty-four hours. The concentrations of Ant and Cis were within the range of 0 - 200 and 0 - 50 µg/mL in MCF7 and $CaCO_2$ cells and within the range of 0 - 500 and 0 - 50 µg/ml in Vero cells, correspondingly. After twenty-four hours of treatment, 10 µL of MTT stock solution (12 mM, 5 mg/mL in sterile PBS) was dispensed into each well, subsequently the plates were incubated at 37°C for 4 extra hours. The MTT solution was subsequently aspirated, and 100 µL of DMSO was added for 20 minutes to dissolve the formazan crystals. The optical density was measured at a wavelength of 570 nm, and cell viability was assessed through the formula:(OD of the treated sample - OD of blank) / (OD of control - OD of blank) × 100%. The experimental data were examined using sigmoidal concentration-response curves, as well as the half-effective inhibitory concentration (IC_{50}) values for Ant and Cis were determined using Graph Pad Prism statistical software [14].

Experimental design

Cells were assigned into four distinct groups: Cnt (untreated control cells), Ant (cells treated with Ant at half of their IC_{50} concentration), Cis (cells treated with Cis at half of their IC_{50} concentration), and Ant+ Cis (cells co-treated with Ant and Cis, each at half of their IC_{50} concentration). Following a 24-hour incubation period under controlled conditions, all cell groups were subjected to RNA isolation and biochemical assays to evaluate the cellular response to treatment.

Caspase 3 activity assay

Cell lysis was performed using Radio-immunoprecipitation assay extraction buffer, and a BSA protein assay reagent was used to measure the total protein concentration, using BSA (Thermo Scientific, USA) as a baseline reference. To assess caspase-3 activity, 200 µM of the caspase-3 fluorogenic substrate (Ac-DEVD-AMC, Alexis Biochemicals, USA) was incubated with 30 µg of the isolated protein using a fluorescent microplate reader set to an excitation wavelength of 405 nm, the substrate's cleavage was identified., providing insights into apoptotic induction in response to treatment.

Intracellular reactive oxygen species detection

Reactive oxygen species (ROS) production was measured utilizing a fluorometric assay based on the oxidative reaction of 2′,7′-dichlorofluorescein diacetate (DCF-DA) into dichlorofluorescein (DCF) [15]. Cells cultured in 96-well plates were allowed to reach 90% confluence before being exposed to Ant or Cis for 24 hours. After treatment, the cells were rinsed twice with PBS and then incubated with 10 µM DCF-DA in fresh medium for 30 minutes. Fluorescence intensity, indicative of intracellular ROS levels, was measured by a

microplate reader with wavelengths of 485 nm for excitation and 535 nm for emission.

Assessment of catalase activity

Catalase (CAT) activity was quantified using a commercial colorimetric hydrogen peroxide (H_2O_2) assay kit (Bio-Diagnostic, Egypt) and as previously detailed [16]. The assay is based on the principle that H_2O_2 exhibits a characteristic UV absorbance at 240 nm, which decreases as it is degraded by CAT. The enzymatic activity was determined by measuring the rate of decline in absorbance. Briefly, 3 mL of Phosphate-H_2O_2 buffer (2 mM) was added to a test tube, this followed by quickly addition of 40 µL of enzyme extract, with immediate mixing. The duration required for the absorbance to reduce by 0.05 units at 240 nm has been measured using a spectrophotometer. A phosphate buffer (0.067 M, pH 7.0) devoid of H_2O_2 was used as a reference. A single unit of CAT activity was described as the amount of enzyme needed for inducing a 0.05-unit reduction in absorbance at 240 nm.

Superoxide dismutase activity detection

The activity of superoxide dismutase (SOD) was determined using a commercial SOD colorimetric kit (Bio-diagnostic, Egypt) [17]. The analysis measures the inhibition of NADH-phenazine methosulfate-nitro blue tetrazolium (NBT) formazan production as an indicator of SOD activity. The final color of the reaction, quantified by spectrophotometric analysis at 560 nm, was extracted into butanol for measurement. The 2.8 ml assay mixture was prepared by combining 0.1 ml of phenazine methosulfate (PMS) with 1.2 ml of sodium pyrophosphate buffer, 0.3 ml of NBT, 0.2 ml of homogenate, and 1.2 ml of water. The reaction was started by adding 2.0 ml of NAD(H), then 3 min incubation at a temperature of 30°C. The reaction was terminated through adding of 1.0 ml of glacial acetic acid. Following this, 4.0 ml of n-butanol was added, the mixture underwent agitation, remain standing for 10 minutes, and centrifuged. The absorbance of colour produced in butanol assessed at 560 nm using a spectrophotometer. The level of inhibition in this process was used to quantify SOD activity. A 50% decrease in NBT reduction within one minute was known as single unit of enzyme activity.

Determination of glutathione peroxidase enzymatic activity

Glutathione peroxidase (GPx) enzyme activity was assessed via a commercial reagent (Bio-diagnostic, Egypt) [18]. The assay is based on the reduction of organic peroxides by GPx, leading to the production of oxidized glutathione (GSSG), which is subsequently recycled to its reduced form by the enzyme glutathione reductase.

Gene expression analysis using RT-PCR

Purification Kit from Thermo Scientific was used to extract total RNA (#K0731) following the manufacturer's protocol. RNA purity and concentration were assessed using a Nanodrop spectrophotometer by measuring absorbance at 260nm ,280 nm, with OD260/OD280 ratios ensuring minimal protein contamination. cDNA was synthesized by RevertAid™ H Minus Reverse Transcriptase (Thermo Scientific). A 25µl reaction mixture was prepared containing the following components: 3 µl of cDNA template (10-20 ng/µl), 12.5 µl of 2X Maxima SYBR Green qPCR Master Mix, 1 µl of each primer (10 µM, Table1), and nuclease-free water. The mixture was loaded into a StepOnePlus real-time thermal cycler, and the PCR program was conducted. The thermal cycling conditions consisted of an initial denaturation step at 95°C for 10 minutes, followed by 40 cycles of denaturation at 95°C for 15 seconds, annealing at 60°C for 30 seconds, and extension at 72°C for 30 seconds. By normalizing to the housekeeping gene (GAPDH), the target gene's relative gene expression or fold change was determined using the 2-ΔΔCt method. Primer sequences were designed using NCBI Primer-BLAST to span exon-exon junctions, and their specificity was confirmed by melt curve analysis. Amplification efficiencies were validated via serial cDNA dilutions (1:10), with efficiencies between 95–105% and $R^2 > 0.99$ for all targets.

Statistical analysis

Statistical analysis was performed using one-way ANOVA with GraphPad Prism 8, followed by Tukey's Honestly Significant Difference as a post hoc test. The mean ± SEM is used to display numerical data. Statistical significance was well-defined at $P < 0.05$.

Results

Effect of Ant and Cis on cell viability

MTT assay results (Fig. 1) showed that Ant had a significant increase in cytotoxicity on $CaCO_2$ and MCF7 with IC50 values of 43.3 ± 3.68 µg/mL and 31.86 ± 2.22 µg/mL, respectively, compared to Cis, that demonstrated IC50 values of 14.88 ± 1.77 and 5.589 ± 0.49 µg/mL, respectively. On the other hand, in Vero cells Ant showed markedly reduced cytotoxicity with (IC50 values of 526.2 ± 32.25 µg/mL) relative to Cis (IC50 values of 98.54± 7.54 µg/mL).

Impact of Ant and Cis on oxidative stress

To investigate the potential of Ant in modulating Cis-induced oxidative stress in cancer cells, we examined the effects of Ant on Cis-mediated ROS generation and antioxidant enzyme inhibition and the experiment showed that Cis resulted in a significant increase in intracellular ROS levels and a significant

decrease in activities of antioxidant enzyme (SOD, CAT, GPx). ROS level was significantly decreased, and the activities of the antioxidant enzymes were significantly increased after treatment Ant alone or in combination with Cis. On the other hand, no significant changes were observed between Cnt and Ant groups (Table 2).

Influence of Ant and Cis on apoptosis

Cis and/or Ant induced apoptosis of $CaCO_2$ and MCF7 cells via triggering a significant increase in caspase-3 activity compared to the control (Cnt) group (Fig. 2). Ant+Cis led to the highest increase in caspase-3 activity compared to all other groups, indicating that the combination of the two compounds significantly increases cell death. Additionally, the qPCR analysis revealed significant alterations in apoptotic gene expression following treatment with Cis, Ant and their combination (Ant + Cis) in $CaCO_2$ and MCF7 cells. Bax expression was significantly upregulated in all treated groups compared to controls, with the highest increase observed in the combination (Ant + Cis), indicating a potential synergistic effect (Fig. 3). Conversely, Bcl2, an anti-apoptotic gene, was significantly downregulated in all treated groups, with Cis showing a stronger inhibitory effect than Ant, while the combination treatment resulted in the most pronounced suppression, reinforcing its role in enhancing apoptosis (Fig. 4).

Influence of Ant and Cis on inflammation and angiogenesis

Cis treatment led to a significant upregulation of TNFα, highlighting its apoptotic and inflammatory role. In contrast, Ant treatment downregulated TNFα, suggesting its anti-inflammatory potential (Fig. 4). Interestingly, the combination therapy mitigated Cis-induced TNFα upregulation, indicating that Ant may counteract Cis-mediated inflammation. Similarly, Cis and Ant significantly suppressed VEGF expression, with Cis exerting a stronger inhibitory effect. Notably, the Ant + Cis combination resulted in the greatest suppression of VEGF, suggesting a synergistic anti-angiogenic effect that may further limit tumor vascularization and proliferation (Fig. 5).

Effect of Ant and Cis on migration

Cis and Ant significantly downregulated MMP9, a key enzyme involved in ECM degradation, with the most substantial suppression observed in the Ant + Cis combination (Fig. 5). In parallel, TIMP1, an inhibitor of MMPs, was upregulated in response to all treatments, with the highest increase noted in the combination therapy, reinforcing ECM stability and potentially limiting tumor invasion (Fig. 6).

Effect of Ant and Cis on antioxidant genes

NrF2, a transcription factor involved in antioxidant defence, was significantly upregulated in Ant-treated cells, suggesting its role in activating protective mechanisms against Cis-induced oxidative damage. The combination treatment also led to increased NrF2 expression, effectively counteracting Cis-induced oxidative stress without reducing its anticancer efficacy (Fig. 6). Meanwhile, HO-1, another antioxidant-related gene, was downregulated in Cis-treated cells, amplifying oxidative stress and promoting cancer cell apoptosis. In contrast, Ant markedly increased HO-1 expression, enhancing cellular defense mechanisms against oxidative damage (Fig. 7). Notably, the Ant + Cis combination restored HO-1 expression to a significant extent, balancing Cis-induced toxicity while preserving its anticancer effect.

Discussion

The present study investigated the potential of Ant derived from Rhubarb officinale as an adjuvant to Cis in colorectal ($CaCO_2$) and breast (MCF7) cancer cells. Our findings demonstrate that Ant enhances Cis-induced apoptosis, mitigates oxidative stress, and modulates key genes involved in cancer progression and metastasis. These results align with previous studies on Ant but also provide novel insights into their synergistic mechanisms with Cis, particularly in regulating oxidative stress and extracellular matrix (ECM) remodeling. Our MTT assay revealed that Ant exhibited lower cytotoxicity compared to Cis in cancer cells, while showing minimal toxicity in normal Vero cells. This selective cytotoxicity aligns with [8], who reported that Rhubarb-derived Ant (e.g., emodin, aloe-emodin) preferentially target cancer cells without harming normal cells. However, our IC50 values for Ant were higher than those reported for isolated emodin in MCF7 cells [19], possibly due to differences in extract composition or assay conditions. The reduced toxicity of Ant in normal cells supports its potential as a safer adjunct to Cis, corroborating findings by [20], who noted emodin's ability to protect non-cancerous cells from chemotherapy-induced damage.

The study revealed that the Ant + Cis combination significantly increased caspase-3 activity and Bax expression with significant reduction of Bcl2 expression compared to monotherapies, indicating enhanced apoptosis. This aligns with Yang et al. [21], who demonstrated that Ant-derived-emodin potentiates Cis-induced apoptosis in HepG2 cells. Similarly, Ant-derived-emodin suppresses Bcl2 signaling in MCF7 cells, mirroring our Bcl2 downregulation results [22]. Notably, our study expands on these findings by showing that Ant's pro-apoptotic effects extend to $CaCO_2$ cells, a model less explored in prior Ant research.

Cis alone increased ROS and suppressed antioxidant enzymes (SOD, CAT, GPx), whereas Ant

counteracted these effects, restoring redox balance. This contrasts with Li, et al. [10], who found that Ant-derived-emodin enhances Cis-induced ROS in bladder cancer cells to promote cytotoxicity. The apparent discrepancy between our observation of Ant reducing ROS levels and Li et al., (2016) reporting ROS induction by Ant can be attributed to several factors, including cell-type specificity, experimental design, and extract composition. Li et al. (2016) demonstrated ROS induction by Ant in HCC cells, where elevated basal ROS levels render cells vulnerable to further oxidative stress. In contrast, our study utilized $CaCO_2$ and MCF7 cancer cells, which may exhibit distinct redox profiles. For instance, MCF7 cells are known to express higher baseline antioxidant defenses (e.g., GPx) compared to HCC models, potentially enabling Ant to counteract Cis-induced ROS without overwhelming cellular redox buffers. This cell-type variability underscores the context-dependent role of ROS in cancer therapy. Cis alone generates significant ROS as part of its cytotoxic mechanism. In our study, Ant co-treatment may have paradoxically attenuated Cis-driven oxidative stress by upregulating antioxidant enzymes (SOD, CAT, GPX) and Nrf2/HO-1 pathways, thereby restoring redox balance. By contrast, Li et al. (2016) examined Ant monotherapy, where ROS elevation likely served as the primary pro-apoptotic trigger. This suggests that Ant's role in ROS modulation shifts from stressor to mitigator depending on the therapeutic context (monotherapy vs. combination). The Rhubarb officinale extract used here contains a unique ratio of emodin, aloe-emodin, and chrysophanol, whereas Li et al. (2016) employed purified emodin. Chrysophanol, in particular, has been shown to activate Nrf2-mediated antioxidant responses in colorectal models, which may dominate in our extract, counterbalancing the ROS-inducing effects of other constituents. Standardization of anthraquinone ratios and further isolation studies are needed to clarify this interplay. ROS modulation by Ant may follow a biphasic pattern: lower doses or shorter exposure times (as in combination therapies) could activate antioxidant pathways to promote cell survival under chemotherapy stress, while higher doses (as in monotherapy studies) may exceed redox buffering capacity, inducing lethal ROS accumulation. Our dosing regimen (optimized for synergy with cisplatin) likely resides in the former range. Our data suggest that Ant dual role, ameliorating Cis toxicity in normal cells while maintaining anticancer efficacy, parallels Akkol, et al. [20], who proposed emodin as a redox modulator. The upregulation of Nrf2 and HO-1 by Ant further supports its cytoprotective potential, a mechanism underexplored in earlier Cis combination studies.

Both Ant and Cis suppressed VEGF and MMP9 while upregulating TIMP1, suggesting synergistic inhibition of metastasis. Liu, et al. [23] reported similar effects with emodin in MCF7 cells, linking MMP9 downregulation to EMT inhibition. Our study extends this to $CaCO_2$ cells, highlighting Ant broad-spectrum anti-metastatic potential. The greater suppression of VEGF by the Ant + Cis combination aligns with Cheng, et al. [24], who observed that aloe-emodin enhances chemotherapy efficacy by blocking angiogenesis. The downregulation of inflammatory markers (TNFα) and upregulation of Nrf2 by Ant may mitigate Cis resistance, a finding consistent with Galluzzi, et al. [25], who identified oxidative stress and inflammation as key resistance drivers. However, unlike Cheng etal. [26], who focused on MDR1 inhibition, our study implicates TIMP1 and HO-1 as novel targets for resensitizing cancer cells to Cis.

This study has several limitations that should be considered when interpreting the results. First, the use of a crude Ant extract rather than purified compounds makes it difficult to determine which specific Ant (e.g., emodin, aloe-emodin) are responsible for the observed effects. Second, the research was conducted exclusively in vitro using only two cancer cell lines ($CaCO_2$ and MCF7), which may not fully represent the complexity of tumors in vivo or other cancer types. Third, while we demonstrated Ant ability to mitigate Cis-induced oxidative stress in normal cells, its paradoxical effects on ROS in cancer cells require further investigation. Additionally, the short duration of our experiments may have missed potential long-term adaptive responses or resistance mechanisms. Finally, the lack of in vivo data limits our understanding of the pharmacokinetics and potential systemic effects of the Ant+Cis combination. Future work could first evaluate the Ant+Cis combination in murine xenograft models using $CaCO_2$ and MCF7 cells to assess tumor growth inhibition, metastasis suppression, and systemic toxicity (renal/hepatic function, body weight). Pharmacokinetic studies could then characterize the bioavailability, tissue distribution, and clearance of Ant constituents alongside Cis, identifying potential synergies or antagonisms. Subsequent toxicity profiling in rodent models could test Ant's protective effects against Cis-induced organ damage using biomarkers like serum creatinine and ALT/AST. To enhance clinical relevance, patient-derived xenografts could be employed to validate efficacy across heterogeneous tumors. Together, these steps could systematically validate the safety and efficacy of Ant+Cis in living systems, bridging our in vitro results toward translational application.

Conclusions

Our study provides compelling evidence that Rhubarb officinale-derived anthraquinones can enhance the therapeutic efficacy of cisplatin while reducing its adverse effects. The Ant+Cis combination demonstrated synergistic anti-cancer

activity by promoting apoptosis through caspase-3 activation and Bax/Bcl-2 modulation, restoring redox balance via Nrf2/HO-1 upregulation, and inhibiting metastatic potential through VEGF and MMP9 suppression. Particularly noteworthy is Ant's selective cytotoxicity, which preferentially targeted cancer cells while showing minimal toxicity in normal Vero cells. The results suggest that Ant could be developed as a promising adjuvant to cisplatin therapy, potentially improving treatment outcomes while reducing side effects. Future studies should focus on isolating active compounds, investigating in vivo models, and exploring clinical applications of this combination therapy.

Acknowledgement

The authors would like to thank faculty of science, Mansoura university for their valuable support and contribution to this study.

Conflicts of interest

There are no conflicts to declare.

Funding statement:

This study received no external funding.

Ethical approval:

This study did not involve human or animal subjects. We used only cell lines.

TABLE 1. Forward and reverse primers sequence for candidate genes

Gene	Forward prime (/5 ------ /3)	Reverse prime (/5 ------ /3)
Bax	ACACCTGAGCTGACCTTG	AGCCCATGATGGTTCTGATC
Bcl2	AGTACCTGAACCGGCATCTG	CATGCTGGGGCCATATAGTT
TNFα	CCCAGGGACCTCTCTCTAATC	CCCAGGGACCTCTCTCTAATC
VEGF	GATCATGCGGATCAAACCTCACC	CCTCCGGACCCAAAGTGCTC
MMP9	TCGAAGGCGACCTCAAGTG	TTCGGTGTAGCTTTGGATCCA
TIMP	CGCAGCGAGGAGGTTTCTCAT	GGCAGTGATGTGCAAATTTCC
Nrf2	CACATCCAGACAGACACCAGT	CTACAAATGGGAATGTCTCTGC
HO-1	GGAAAGCAGTCATGGTCAGTCA	CCCTTCCTGTGTCTTCCTTTGT
GAPDH	GGTGAAGGTCGGAGTCAACG	TGAAGGGGTCATTGATGGCAAC

TABLE 2. Effect of Ant and/or CIS on ROS, SOD, CAT and GPX levels in $CaCO_2$ and MCF7 cell line.

Groups	Cell line	ROS	SOD	CAT	GPX
		(% of control)			
Cnt	**$CaCO_2$**	100.95 ± 5.3 [a]	101.35 ± 3.29 [a]	100.27 ± 4.28 [a]	101.53 ± 5.59 [a]
Ant		102.75 ± 3.59 [b]	104.17 ± 5.8 [b]	107.03 ± 5.76 [b]	109.65 ± 8.20 [b]
Cis		246.0 ± 7.19 [c]	39.25 ± 2.39 [c]	33.6 ± 2.71 [c]	14.16 ± 1.26 [c]
Ant+Cis		150.74 ± 8.34 [d]	77.82 ± 4.39 [d]	61.64 ± 3.16 [d]	33.56 ± 2.79 [d]
Cnt	**MCF7**	101.31 ± 3.07 [a]	100.21 ± 2.04 [a]	101.26 ± 2.49 [a]	101.37 ± 1.43 [a]
Ant		95.96 ± 4.15 [b]	105.82 ± 3.61 [b]	106.50 ± 3.18 [b]	104.99 ± 3.42 [b]
Cis		199.53 ± 7.27 [c]	50.66 ± 3.12 [c]	39.15 ± 2.55 [c]	22.72 ± 1.74 [c]
Ant+Cis		152.08 ± 5.6 [d]	80.88 ± 3.35 [d]	77.74 ± 2.8 [d]	45.15 ± 1.97 [d]

Data were presented as means ± SEM (n = 5). Means within the same column carrying different superscript letters [a (the highest value) – d (lowest value)] denote significant results at $p < 0.05$.

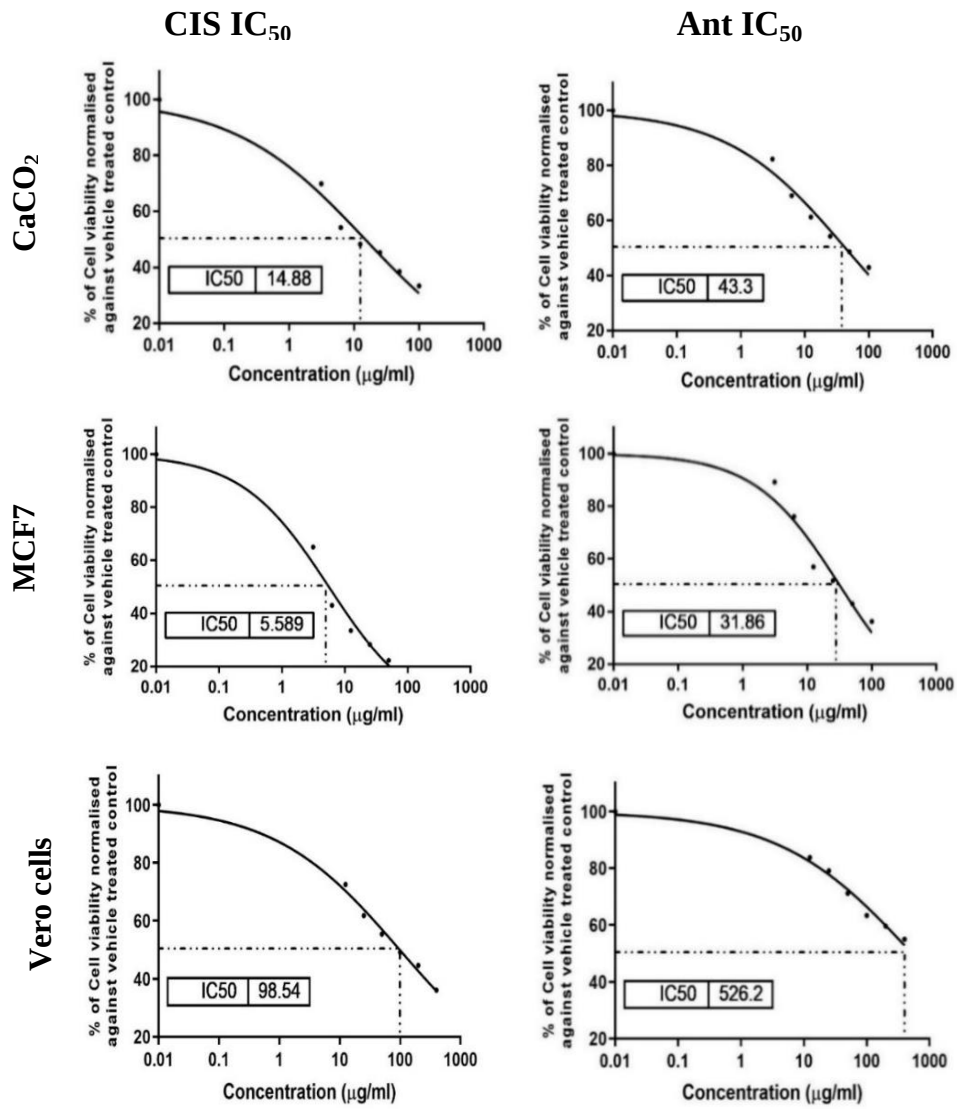

Fig. 1. MTT assay results showed IC50 of Ant and Cis on in $CaCO_2$, MCF7 and Vero cel

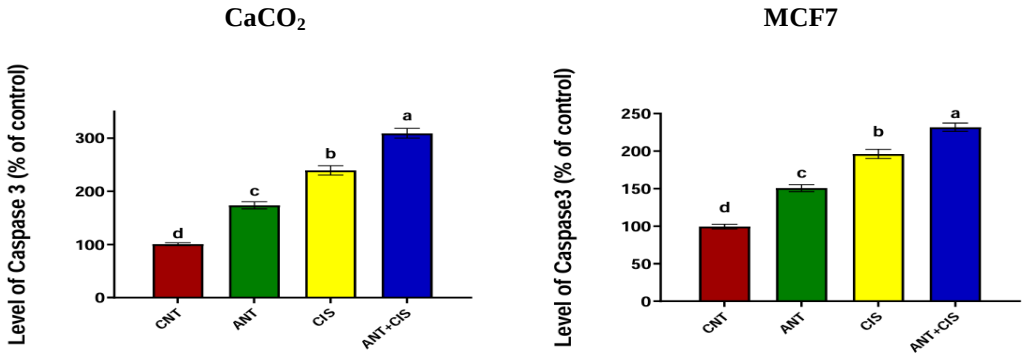

Fig. 2. Graphical presentation of level of caspase3 (% of control) of Cis, Ant, and Cis + Ant extract on MCF7 and $CaCO_2$ cells. Means within the same column carrying different letters [a (the highest value, d (the lowest value)] are significantly different at P≤ 0.05.

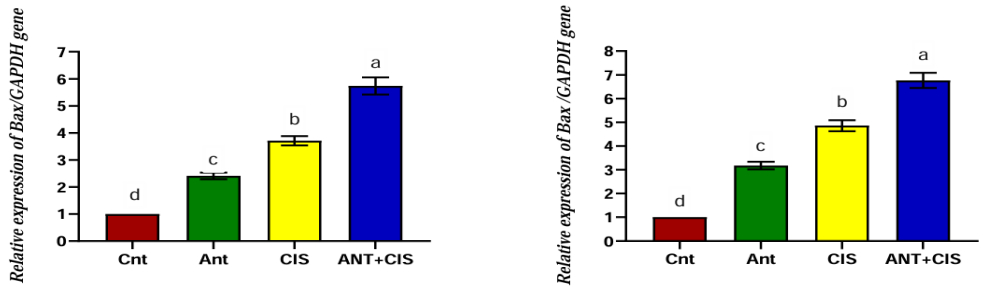

Fig. 3. Graphical presentation of real-time quantitative PCR analysis of the expression of Bax in $CaCO_2$ and MCF7 cells following treatments with Ant and/or Cis. Means within the same column carrying different superscript letters [a (the highest value, d (the lowest value)] are significantly different (P≤ 0.05).

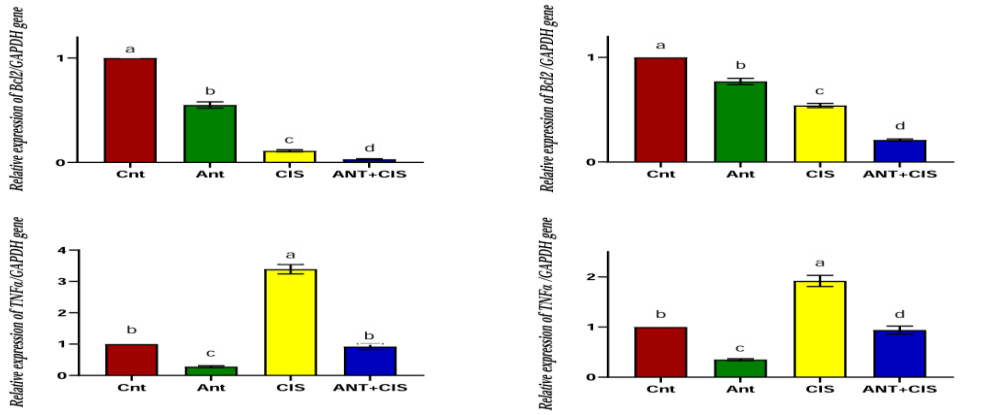

Fig. 4. Graphical presentation of real-time quantitative PCR analysis of the expression of Bcl2 and TNFα in $CaCO_2$ and MCF7 cells following treatments with Ant and/or Cis. Means within the same column carrying different superscript letters [a (the highest value, d (the lowest value)] are significantly different (P≤ 0.05).

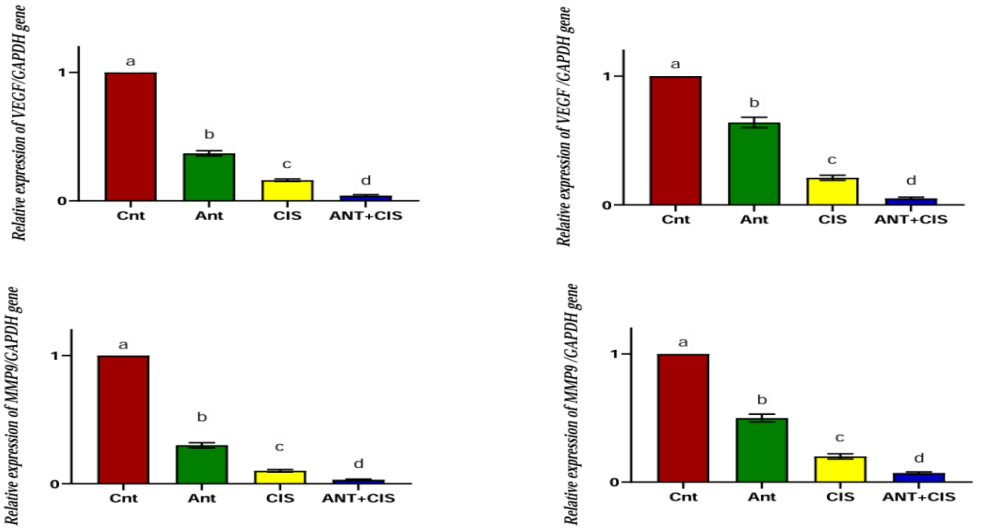

Fig. 5. Graphical presentation of real-time quantitative PCR analysis of the expression of VEGF and MMP9 in $CaCO_2$ and MCF7 cells following treatments with Ant and/or Cis. Note: Means within the same column carrying different superscript letters [a (the highest value, d (the lowest value)] are significantly different (P≤ 0.05).

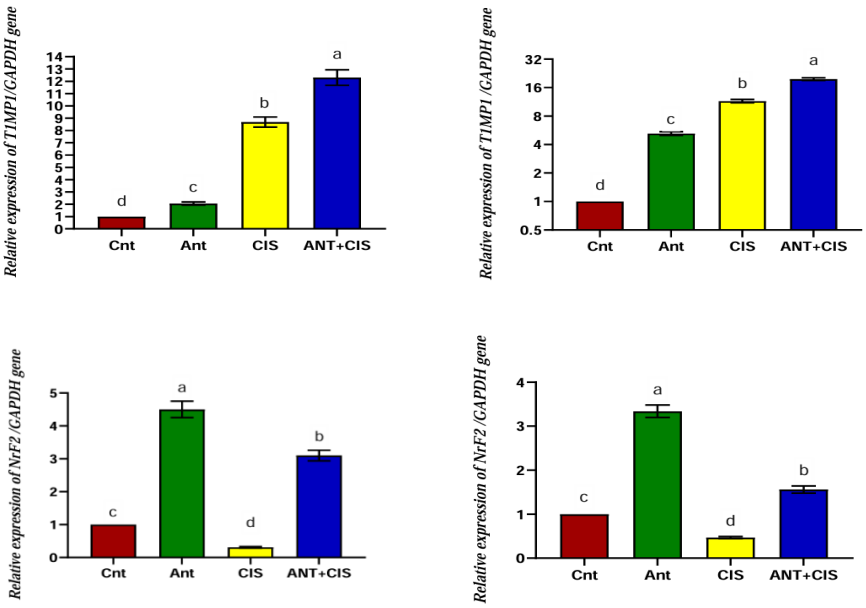

Fig. 6. Graphical presentation of real-time quantitative PCR analysis of the expression of TIMP1 and NrF2 in $CaCO_2$ and MCF7 cells following treatments with Ant and/or Cis. Note: Means within the same column carrying different superscript letters [a (the highest value, d (the lowest value)] are significantly different (P≤ 0.05).

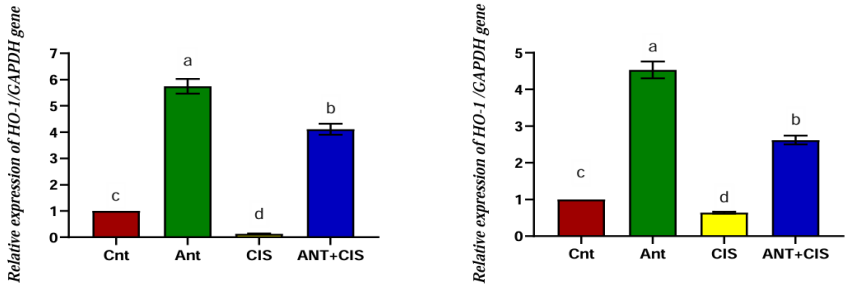

Fig. 7. Graphical presentation of real-time quantitative PCR analysis of the expression of HO-1 in $CaCO_2$ and MCF7 cells following treatments with Ant and/or Cis. Note: Means within the same column carrying different superscript letters [a (the highest value, d (the lowest value)] are significantly different (P≤ 0.05).

References

1. Tawfic, A.A., Ibrahim, H.M., Mohammed-Geba, K. and Abu El-Magd, M. Immunomodulatory Effect of Chitosan Nanoparticles on Ehrlich Ascites Carcinoma Mice. *Egyptian Journal of Veterinary Sciences.*, 1-9, (2024). DOI:10.21608/ejvs.2024.331998.2455,
2. Awad, M.G., Hanafy, N.A.N., Ali, R.A., El-Monem, D.D.A., El-Shafiey, S.H. and El-Magd, M.A. Unveiling the therapeutic potential of anthocyanin/cisplatin-loaded chitosan nanoparticles against breast and liver cancers. *Cancer Nanotechnology*, **15**, 57 (2024).
3. Minarni, Artika, I.M., Julistiono, H., Bermawie, N., Riyanti, E.I. and Hasim, Hasan, A.E.Z. Anticancer activity test of ethyl acetate extract of endophytic fungi isolated from soursop leaf (Annona muricata L.). *Asian Pacific journal Of Tropical Medicine*, **10**, 566-571(2017).
4. Dai, W., Xu, X., Wang, D., Wu, J. and Wang, J. Cancer therapy with a CRISPR-assisted telomerase-activating gene expression system. *Oncogene*, **38**, 4110-4124, (2019).
5. Tawfic, A.A., Ibrahim, H.M., Mohammed-Geba, K. and El-Magd, M.A. Chitosan nanoparticles, camel milk exosomes and/or Sorafenib induce apoptosis, inhibit tumor cells migration and angiogenesis and ameliorate the associated liver damage in Ehrlich ascites carcinoma-bearing mice. *Beni-Suef University Journal of Basic and Applied Sciences*, **13**, 74, (2024).
6. Abass, S.A., Elgazar, A.A., El-kholy, S.S., El-Refaiy, A.I., Nawaya, R.A., Bhat, M.A., Farrag, F.A., Hamdi, A., Balaha, M. and El-Magd, M.A. Unraveling the Nephroprotective Potential of Papaverine against Cisplatin Toxicity through Mitigating Oxidative Stress and Inflammation: Insights from In Silico, In Vitro, and In Vivo Investigations. In *Molecules*, **29**(9),1927.(2024)

7. Siddik, Z.H. Cisplatin: mode of cytotoxic action and molecular basis of resistance. *Oncogene*, **22**, 7265-7279, (2003).

8. Huang, Q., Lu, G., Shen, H.M., Chung, M.C. and Ong, C.N. Anti-cancer properties of anthraquinones from rhubarb. *Medicinal research Reviews*, **27**, 609-630 (2007).

9. Xing, Y.X., Li, M.H., Tao, L., Ruan, L.Y., Hong, W., Chen, C., Zhao, W.L., Xu, H., Chen, J.F. and Wang, J.S. Anti-Cancer Effects of Emodin on HepG2 Cells as Revealed by (1)H NMR Based Metabolic Profiling. *Journal of Proteome Research*, **17**, 1943-1952, (2018).

10. Li, X., Wang, H., Wang, J., Chen, Y., Yin, X., Shi, G., Li, H., Hu, Z. and Liang, X. Emodin enhances cisplatin-induced cytotoxicity in human bladder cancer cells through ROS elevation and MRP1 downregulation. *BMC Cancer*, **16**, 578, (2016).

11. Malik, M.S., Alsantali, R.I., Jassas, R.S., Alsimaree, A.A., Syed, R., Alsharif, M.A., Kalpana, K., Morad, M., Althagafi, II. and Ahmed, S.A. Journey of anthraquinones as anticancer agents - a systematic review of recent literature. *RSC Advances*, **11**, 35806-35827, (2021).

12. Selim, N.M., Elgazar, A.A., Abdel-Hamid, N.M., El-Magd, M.R.A., Yasri, A., Hefnawy, H.M.E. and Sobeh, M. Chrysophanol, Physcion, Hesperidin and Curcumin Modulate the Gene Expression of Pro-Inflammatory Mediators Induced by LPS in HepG2: In Silico and Molecular Studies. *Antioxidants*, **8**, 371 (2019).

13. Al-Mathal, E.M., Khaffagy, A.E. and Abu El-Magd, M. Evaluation of Four Herbicides Cytotoxicity on Normal Liver THLE2 Cells. *Egyptian Journal of Veterinary Sciences*, **55**, 881-894 (2024).

14. Awad, M.G., Hanafy, N.A.N., Ali, R.A., Abd El-Monem, D.D., El-Shafiey, S.H. and El-Magd, M.A. Exploring the therapeutic applications of nano-therapy of encapsulated cisplatin and anthocyanin-loaded multiwalled carbon nanotubes coated with chitosan-conjugated folic acid in targeting breast and liver cancers. *International Journal of Biological Macromolecules*, **280**, 135854 (2024).

15. Elsied, M.A., Sharawi, Z.W., Al-Amrah, H., Hegazy, R.A., Mohamed, A.E., Saleh, R.M., El-kholy, S.S., Farrag, F.A., Fayed, M.H. and El-Magd, M.A. Walnut Kernel Oil and Defatted Extracts Enhance Mesenchymal Stem Cell Stemness and Delay Senescence. *Molecules*, **28**, 6281 (2023).

16. El-Shazly, S.A., Alhejely, A., Alghibiwi, H.K., Dawoud, S.F.M., Sharaf-Eldin, A.M., Mostafa, A.A., Zedan, A.M.G., El-Sadawy, A.A. and El-Magd, M.A. Protective effect of magnetic water against AlCl3-induced hepatotoxicity in rats. *Scientific Reports*, **14**, 24999, (2024).

17. AbdAllah, O., Gwailly, M.S., Awad, A. and Abu El-Magd, M. Biochemical and Molecular Changes Associated with Asthenozoospermia. *Egyptian Journal of Veterinary Sciences*, **55**, 705-713 (2024).

18. Zedan, A.M.G., Sakran, M.I., Bahattab, O., Hawsawi, Y.M., Al-Amer, O., Oyouni, A.A.A., Nasr Eldeen, S.K. and El-Magd, M.A. Oriental Hornet (Vespa orientalis) Larval Extracts Induce Antiproliferative, Antioxidant, Anti-Inflammatory, and Anti-Migratory Effects on MCF7 Cells. *Molecules*, **26**,3303(2021). ,https://doi.org/3310.3390/molecules26113303,

19. Li, S., Lin, J., Wei, J., Zhou, L., Wang, P. and Qu, S. Sinigrin impedes the breast cancer cell growth through inhibition of PI3K/AKT/mTOR phosphorylation-mediated cell cycle arrest. *Journal of Environmental Pathology, Toxicology and Oncology*, **41**(3), 33-43.(2022).

20. Akkol, E.K., Tatlı, II, Karatoprak, G., Ağar, O.T., Yücel, Ç., Sobarzo-Sánchez, E. and Capasso, R. Is Emodin with Anticancer Effects Completely Innocent? Two Sides of the Coin. *Cancers*, **13**(11), 2733(2021).

21. Yang, M., Xiong, Z., Deng, H., Chen, X., Lai, Q., Wang, H. and Leng, Y. Effect of emodin combined with cisplatin on the invasion and migration of HepG2 hepatoma cells. *Journal of physiology and pharmacology : An Official Journal of the Polish Physiological Society*, **74**(4), 04(2023).

22. Sui, J.Q., Xie, K.P., Zou, W. and Xie, M.J. Emodin inhibits breast cancer cell proliferation through the ERα-MAPK/Akt-cyclin D1/Bcl-2 signaling pathway. *Asian Pacific journal Of Cancer Prevention : APJCP*, **15**, 6247-6251 (2014).

23. Liu, Q., Hodge, J., Wang, J., Wang, Y., Wang, L., Singh, U., Li, Y., Yao, Y., Wang, D., Ai, W., Nagarkatti, P., Chen, H., Xu, P., Murphy, E. A. and Fan, D. Emodin reduces Breast Cancer Lung Metastasis by suppressing Macrophage-induced Breast Cancer Cell Epithelial-mesenchymal transition and Cancer Stem Cell formation. *Theranostics*, **10**, 8365-8381, (2020).

24. Cheng, G., Pi, Z., Zhuang, X., Zheng, Z., Liu, S., Liu, Z. and Song, F. The effects and mechanisms of aloe-emodin on reversing adriamycin-induced resistance of MCF-7/ADR cells. *Phytotherapy research : PTR*, **35**, 3886-3897 (2021).

25. Galluzzi, L., Senovilla, L., Vitale, I., Michels, J., Martins, I., Kepp, O., Castedo, M. and Kroemer, G. Molecular mechanisms of cisplatin resistance. *Oncogene*, **31**, 1869-1883 (2012).

26. Cheng, Q., Liao, M., Hu, H., Li, H. and Wu, L. Asiatic Acid (AA) Sensitizes Multidrug-Resistant Human Lung Adenocarcinoma A549/DDP Cells to Cisplatin (DDP) via Downregulation of P-Glycoprotein (MDR1) and Its Targets. *Cellular physiology and biochemistry : International Journal Of Experimental Cellular Physiology, Biochemistry, And Pharmacology*, **47**, 279-292 (2018).

تقييم التأثير المضاد للسرطان للأنثراكينونات على خلايا سرطان القولون المستقيمى والثدى البشريه

مصطفى أ.الصاوى، محمد عمرو المسيرى،ماجي أ.امير ومحمد أ.المجد*

قسم علم الحيوان ، كليه العلوم جامعه المنصورة ، المنصورة ، مصر.

الملخص

يستخدم عقار السيسبلاتين على نطاق واسع كعامل مضاد للسرطان لعلاج انزاع مختلفه من الاورام بما فى ذلك سرطانات الكبد والثدي والقولون المستقيمى والبنكرياس. ومع ذلك، فإن استخدامه مقيد بسبب آثاره الجانبية، والتي تشمل عدم الانتقائية وتلف الحمض النووي لكل من الخلايا السرطانية والسليمة. هدفت هذه الدراسة إلى تقييم التأثير العلاجي لمركبات الأنثراكينون (ANT) المستخلصه من نبات الراوند الطبي ضد خلايا سرطان القولون المستقيمى ($CaCO_2$) وخلايا سرطان الثدى (MCF7) . قُسّمت الخلايا إلى أربع مجموعات: المجموعة الضابطة (خلايا غير معالجة)، مجموعة (خلايا عُولجت بالأنثراكينونات فقط)، مجموعة (خلايا عُولجت بالسيسبلاتين فقط)، والمجموعة الرابعة (خلايا عُولجت بمزيج من السيسبلاتين والأنثراكينونات). وأظهرت النتائج ان العلاج بالانثراكينونات او المزيج من الانثراكينونات + السيسبلاتين حفز موت الخلايا المبرج فى خلايا الثدى والقولون المستقيمى عن طريق الزياده فى نشاط انزيم (Caspase – 3) و جين (Bax) وانخفاض كبير فى جين (Bcl2) . كما أدى الى إلى تقليل تعبير جينات (TNFα, VEGF, MMP9) بينما زاد من تعبير جين (T1MP1). فيما يتعلق بالاجهاد التأكسدى فقد ادى الى زياده نشاط (SOD, CAT, GPX) زيادة نشاط الإنزيمات المضادة للأكسدة (NrF2 and HO-1).تخلص الدراسه ان الجمع بين الامثراكينونات والسيسبلاتين عزز بشكل فعال الفعالية المضادة للورم لسيسبلاتين مع تقليل السمية الناجمة عن العلاج الكيميائي والحفاظ على السلامة الخلوية.

الكلمات الدالة: الانثراكينونات، السيسبلاتين، خلايا سرطان الثدى MCF7 ، خلايا سرطان القولون المستقيمى $CaCO_2$ ، موت الخلايا المبرمج.